

Somatostatinoma: collision with neurofibroma and ultrastructural features

W. Varikatt, J.L.C. Yong and M.C. Killingsworth

Department of Anatomical Pathology, South Western Area Pathology Service, Sydney, Australia

Summary. The clinical presentation, histopathology and immunoelectron microscopic features of two cases of duodenal somatostatinoma are described, one of which is a hitherto unreported example of a collision tumour with a neurofibroma. Ultrastructural morphometric immunoelectron microscopy studies revealed the presence of four types of cells in both tumours, but there was no difference in the proportions of these cells between the collision tumour and the non-collision tumour. Neurosecretory granules ranging in size from 255-815 nm were generally larger than those previously reported for somatostatinomas and somatostatin was identified in granules of all sizes across this range. Neither tumour was associated with the somatostatinoma syndrome comprising associated diabetes mellitus, steatorrhoea and cholelithiasis.

Key words: Somatostatinoma, Neurofibromatosis, Duodenum, Electron microscopy

Introduction

Somatostatinomas are uncommon neuroendocrine tumours found in the periampullary region of the duodenum or pancreas. Those arising in the pancreas may be associated with the somatostatinoma syndrome of diabetes mellitus, steatorrhoea and cholelithiasis (Dayal and Ganda 1991, Mao et al., 1995) but the syndrome has not been reported for the duodenal variant.

Whereas up to 50% of somatostatinomas of the duodenum are associated with neurofibromatosis, none have to date been reported as a collision tumour association. The clinical presentation, macroscopic and microscopic appearances of each tumour is described, and the electron microscopic and immunoelectron

microscopic identification of somatostatin granules in the neurosecretory apparatus of the cells was assessed semi-quantitatively.

Materials and methods

Case 1

A female, 37-year-old patient, presented with abdominal pain and obstructive jaundice. She had a past history of cholecystectomy for gallstones when a diagnosis of Type I neurofibromatosis was established. There were no features of somatostatinoma syndrome. She was also hypothyroid. There was no relevant family history. Investigations on her admission to hospital showed total serum bilirubin to be 40 $\mu\text{mol/L}$ (normal range 0-18 micromol/L), alkaline phosphatase was 9.30 μL (normal range 6-46 μL) raised gamma GT, AST, ALT and slightly raised blood glucose. There were no investigations such as serum somatostatin or by-products to confirm the diagnosis of somatostatinoma, as the diagnosis was not suspected. Upper gastroenteroscopy showed a large ampullary mass and ultrasound examination showed a dilated common bile duct. Biopsy of the mass was reported as non-diagnostic, with unusual Brunner's glands. The patient underwent a Whipple's procedure with an intraoperative frozen section diagnosis of somatostatinoma.

The macroscopic specimen included the distal stomach, duodenum and head of the pancreas. In the region of the ampulla of Vater was a large tumour 35x22x17 mm (Fig. 1) with intact mucosa over it, a greyish cut surface and a firm, rubbery consistency. The common bile duct was markedly dilated and there was a second nodule 20x15x15 mm at the site of the accessory duct opening.

Case 2

A 54-year-old Italian woman presented in 1998 with recent onset of vague abdominal symptoms. Blood tests

revealed a biliary obstructive picture with high alkaline phosphatase. Her only relevant past history included von Recklinghausen's disease and slightly elevated blood cholesterol. She underwent an ERCP which showed a nodular tumour in the second part of duodenum adjacent to the ampulla. A diagnosis of somatostatinoma was established on biopsy. She underwent a Whipple's procedure.

The macroscopic specimen included a segment of duodenum with the attached head of pancreas. Well away from the resection margins, adjacent to the ampulla, was an ill defined, rubbery tumour with a grey/white, cut surface 10x9x7 mm which was confined to the bowel wall.

She was well five years after her Whipple's operation without evidence of recurrence or metastasis. A year ago she underwent total hysterectomy for post-menopausal bleeding. The cervix was found to contain many neurofibromata and there was a Brenner tumour in the right ovary.

Samples of the tumours in both cases were fixed in 10% buffered formalin and embedded in paraffin. Routine haematoxylin and eosin stained sections were prepared for initial examination and were then followed by immunohistochemical investigations for synaptophysin (DakoCytomation, Denmark), chromogranin A (DakoCytomation, Denmark), somatostatin (DakoCytomation, USA), insulin (DakoCytomation, USA), glucagon (DakoCytomation, USA), gastrin (DakoCytomation, USA), pancreatic polypeptide (DakoCytomation, USA), S-100 (Lipshaw, USA) and CD-34 (DakoCytomation, Denmark). Antigen labelling was visualised using the LSAB2 link system followed by reaction with 3,3'-diaminobenzidine (DAB) chromogen performed in an Autostainer universal staining system (Dako, Denmark).

Processing of tissue for electron microscopy was routine using a standard method (Johannessen, 1973) with some extended times. Block staining with 2% osmium tetroxide and 2% uranyl acetate was carried out prior to dehydration and infiltration with Spurr resin. Ultrathin sections were cut at 130 nm and stained with uranyl acetate and lead citrate. Digital images were acquired at 80 kV using a MegaView III CCD camera (Soft Imaging System GmbH, Germany) integrated with a Morgagni 268D transmission electron microscope (FEI, The Netherlands).

Immunoelectron microscopy was carried out using a standard method (Stirling and Graff, 1995) with some modifications as follows. Antigen retrieval was carried out by floating the grids on a pre-heated retrieval solution that was maintained at 95°C for 20 minutes in a REM microwave oven (Milestone S.r.l, Italy). The grids were then incubated on primary antibody to somatostatin followed by a protein-A gold conjugate (Auroprobe, USA). Negative control grids were treated identically to above except for incubation on antibody diluent only (DakoCytomation, Denmark) rather than antibody to somatostatin.

Somatostatinoma cells in both cases were enumerated in 50 standard electron microscopy fields defined by the grid bars of a 200-mesh hexagonal pattern thin-bar specimen grid. Nuclear, cytoplasmic and membrane features and the structural relationship of different cell types as well as the density of the various cell types were noted.

We also carried out a semi-quantitative analysis of cytoplasmic granule diameter using electron microscopic online image analysis tools in AnalySIS-Pro (Soft Imaging System GmbH, Germany). Images were acquired at 36,000x and arbitrary distance measurements performed using manual cursor placement. Thirty granules were measured from each of three fields representative of cells containing large secretory granules and smaller dense core granules from each case.

Results

Histopathology

Case 1

The bulk of tumour possessed the characteristic features of a somatostatinoma including uniform cells arranged in cords and acini. The tumour cells displayed small central nuclei with finely stippled chromatin and nucleoli embedded in eosinophilic granular cytoplasm (Fig. 2). There were no mitoses evident and many psammoma bodies were distributed throughout the tumour (Fig. 2). At the base of the somatostatinoma mass was a spindle cell tumour with the features and staining characteristics of a neurofibroma (Fig. 3). The



Fig. 1. Macroscopic view of surgical specimen from Case 1 with main tumour mass in the ampulla of Vater and a smaller adjacent nodule.

Somatostatinoma collision tumour

somatostatinoma was strongly positive for synaptophysin, chromogranin and somatostatin (Fig. 4) and negative for insulin, glucagon, gastrin, pancreatic polypeptide, S-100 and CD34. The spindle cell neurofibroma was positive for S-100 and CD34 (Fig. 5).

Case 2:

This somatostatinoma had a small number of psammoma bodies distributed through it. The tumour arose from the mucosa but infiltrated into the submucosa evoking a desmoplastic reaction. There was lymphatic invasion and metastatic tumour in four lymph nodes.

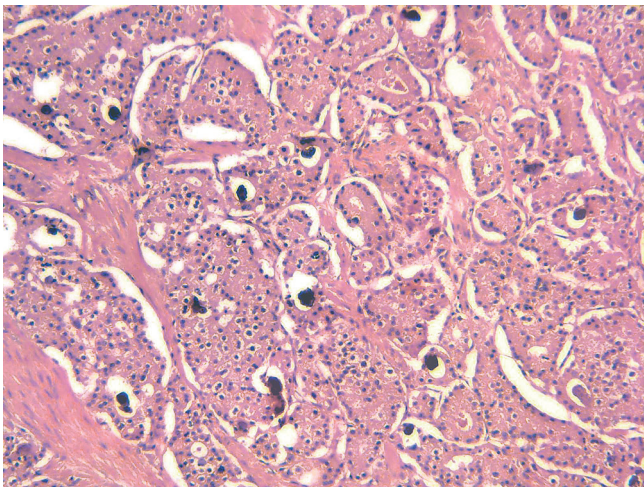


Fig. 2. Somatostatinoma showing typical glandular architecture with many intraluminal psammoma bodies (H&E, x 500).

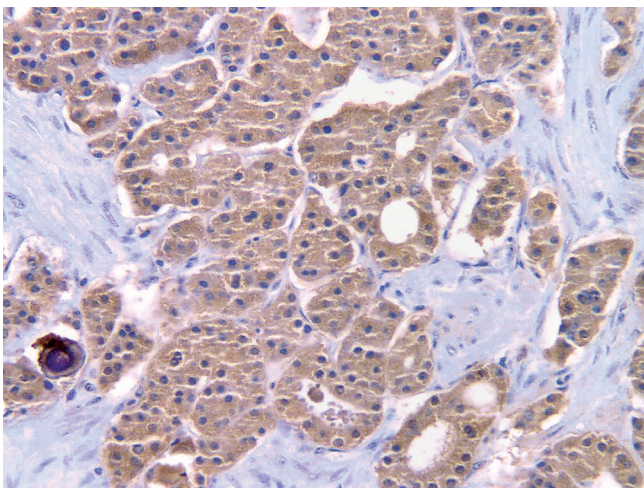


Fig. 4. Somatostatinoma from Case 1 showing strong positive somatostatin immunohistochemical staining. Case 2 somatostatinoma showed similar staining (x 500).

The tumour cells showed positive immunohistochemical staining for chromogranin, synaptophysin and somatostatin.

Electron microscopy

In both cases, somatostatinoma cells formed neoplastic acinar structures commonly encircling a central lumen. Lumina commonly contained electron-dense crystalline material, or psammoma bodies (Fig. 6).

Abundant secretory-like granules of varying size and electron-density characterised most tumour cells observed. These granules were located predominantly in a central perinuclear region. Morphologically and based

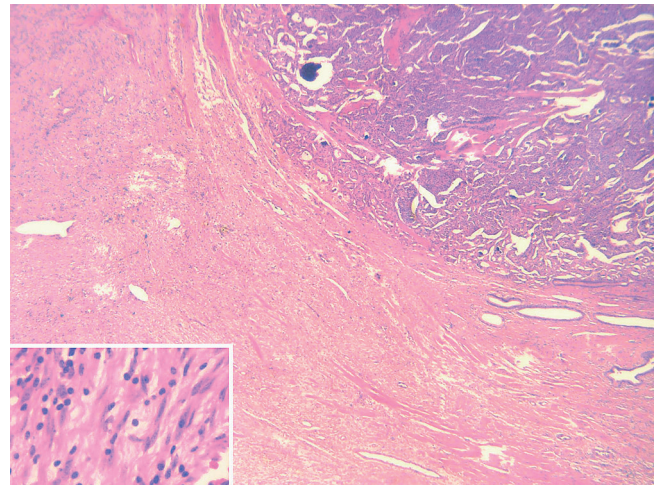


Fig. 3. Region of collision between somatostatinoma and neurofibroma (H&E, x 300). Inset: Shows spindle cells of neurofibroma (H&E, x 500).

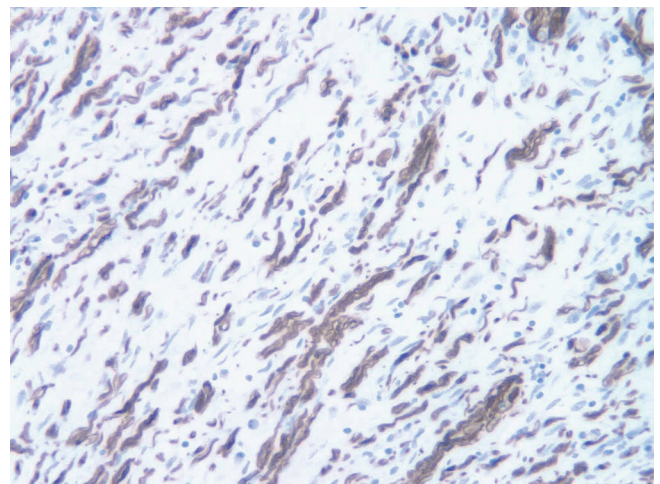


Fig. 5. Neurofibroma showing positive S-100 immunohistochemical staining (x 500).

on the variation in granule appearance we were able to separate the tumour cells into four phenotypes which we have designated types 1 to 4 (Table 1). Type 1 cells accounted for approximately 75% of the tumour. They contained numerous electron-dense granules (Fig. 6). Type 2 cells made up only 8% of total cells and contained a similar number of granules which were less electron-dense (Fig. 7). Type 3 cells made up approximately 16% of total cells and displayed smaller and fewer electron-dense granules. They were found mainly in the periphery of acinar structures and to a lesser extent within central regions (Fig. 7). Type 4 cells accounted for only 0.6% of total cells, contained

occasional small granules similar to type 3 cells and were mainly located in the periphery of acinar structures (Fig. 7).

The bulk of the tumour comprised nests of type 1 and 2 cells. Morphometric analysis of their granule size indicated a mean diameter of 625 nm for Case 1 and 815 nm for Case 2 (Table 2). Granule electron-density appeared to be size related with larger examples generally showing less heavy metal staining. The limiting membrane was usually intact around smaller granules, separated from the finely granular contents by a lucent space giving the appearance of a remnant halo structure (Fig. 8) but the largest granules frequently showed a fragmented limiting membrane. Nuclei of these cells were round to oval with dispersed chromatin

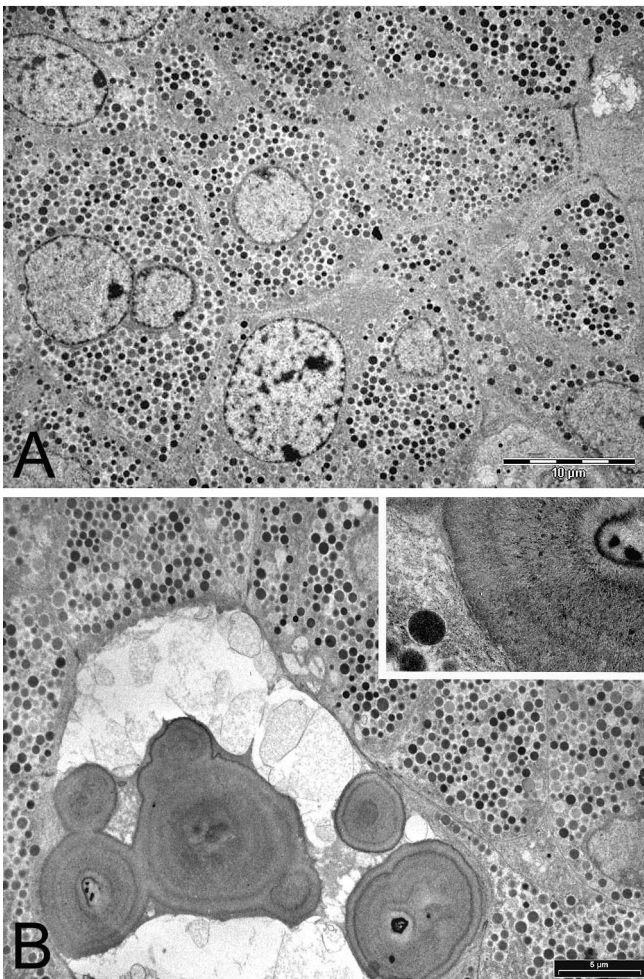


Fig. 6. **A.** Electron microscopic view of somatostatinoma showing tumour cells with abundant cytoplasmic granules dispersed throughout the cytoplasm. Cells such as these made up the major part of the tumour and were classified as type 1. Granules are 625-815 nm in diameter (Osmium, uranium and lead stain, x 1,800). **B.** Somatostatinoma cells bordering a lumen containing a psammoma body composed of concentric layers of electron-dense crystals thought to be calcium apatite (Osmium, uranium and lead stain, x 2,300). Inset: Detail of crystalline material (Osmium, uranium and lead stain, x 11,500).

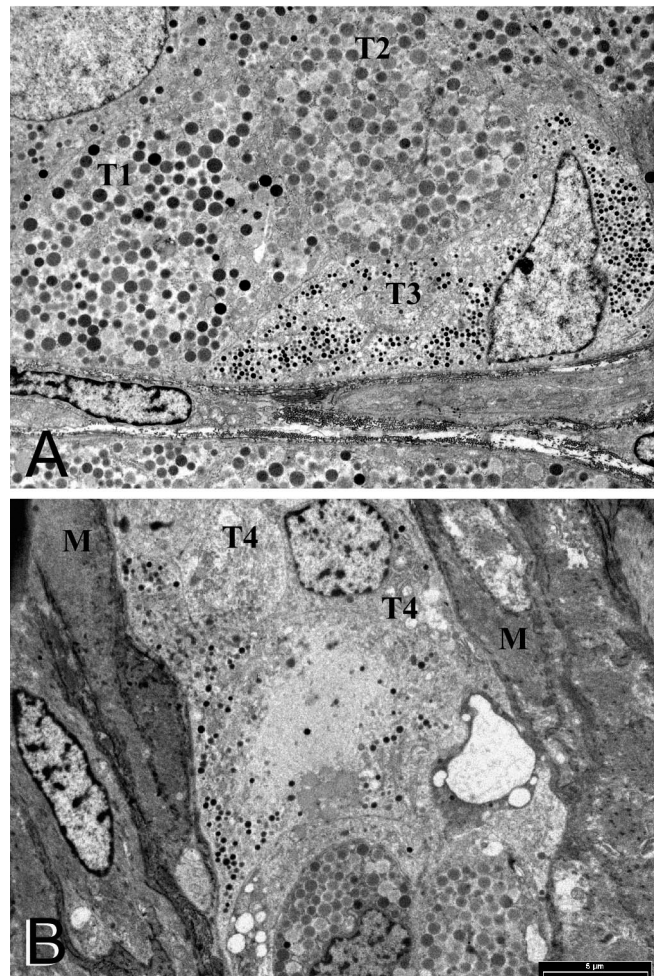


Fig. 7. A subpopulation of somatostatinoma cells designated as types 3 and 4 contained smaller electron-dense 255-433 nm neurosecretory granules. **A.** Type 3 (T3) cell at the periphery of an acinar formation adjacent a type 1 (T1) cell and a type 2 (T2) cell (Osmium, uranium and lead stain, x 2,800). **B.** Type 4 (T4) cells with sparse 255-433 nm cytoplasmic granules forming the leading edge of the tumour inserted between muscle (M) cells (Osmium, uranium and lead stain, x 2,800).

Somatostatinoma collision tumour

and prominent nucleoli, in some cases up to three per nucleus. Mitochondria were elongated and sparse located in the basal cytoplasm. There were cytoplasmic filaments in the periphery with an occasional centriole and a small amount of rough endoplasmic reticulum. There was a thin external basal lamina-like structure that surrounded the nests of cells presumably corresponding to the basement membrane. Stunted apical microvilli were occasionally seen protruding into a luminal space. Neighbouring cells showed junctional zones of cell-to-cell contact comprising poorly developed tight junctions and small desmosome-like structures. Intercellular spaces occasionally showed electron-dense staining which outlined interdigitating blunt cell processes of the lateral cell membrane (Fig. 9). This staining did not outline the whole cell and was seen to terminate at desmosome junctions (Fig. 9).

Type 3 cells appeared to comprise a minor subpopulation of tumour cells observed at the periphery and occasionally in central regions of acini in both cases (Fig. 7). The secretory granules of these cells were more typical in appearance of neuroendocrine granules with intact limiting membranes bordering an electron-lucent halo and electron-dense core (Table 1). Mean granule diameters were 255 nm for Case 1 and 433 nm for Case 2 (Table 2). The cytoplasmic distribution of the granules was regional and they were frequently associated with smooth endoplasmic reticulum (SER), which was more

plentiful in these cells than the cells containing larger secretory granules. Other ultrastructural features of these cells included a round to irregular nuclear outline, a fine layer of basal lamina-like material, prominent regions of cytoplasmic filaments and a moderate amount of rough endoplasmic reticulum (RER).

Type 4 tumour cells resembled type 3 cells but had fewer of the smaller neuroendocrine-like granules and contained well-developed runs of SER (Table 1). They were generally observed at the tumour periphery and were occasionally seen extending between the surrounding stroma and muscle tissue.

Mast cells were also observed in the vicinity of the neoplastic cells and could initially be mistaken for tumour cells because of their similar electron-dense cytoplasmic granules. However, on closer examination the content of these granules was more structured with scroll-like formations rather than the finely granular material of the somatostatinoma cell granules.

Psammoma bodies within luminal spaces were commonly encountered. At low magnification these bodies appeared as irregular electron-dense masses made up of multiple interconnected spherical bodies forming a conglomerate pattern. Individual spherules within the conglomerate mass appeared as concentrically lamellated structures containing crystalline spicules with varying electron density (Fig. 6). Similar though smaller cytoplasmic crystalline deposits were also observed

Table 1. Somatostatinoma tumour cell ultrastructural phenotypes

Tumour cell phenotype	Location	Granule size	Granule appearance	Granule numbers	Other cytoplasmic features	% of total cells
Type 1	Forming bulk of acini	Large	Electron-dense core with intact or fragmented limiting membrane	Frequent	Round nucleus with nucleolus, stunted apical microvilli, terminal bar tight junctions, desmosome-like structures, fine basal lamina-like structure	75.5
Type 2	Forming acini	Large	Pale to moderately electron-dense core with fragmented limiting membrane	Frequent	Same as above but with irregular nucleus	8.0
Type 3	Mainly in periphery of acini and less within central region	Small	Electron-dense core with intact limiting membrane	Few to frequent	Round to irregular nucleus, fine external basal lamina-like structure, prominent SER, moderate amount of RER, desmosome-like junctions with type 1 and 2 cells, areas of cytoplasmic vacuolation associated with granules	15.8
Type 4	Periphery of acini occasionally protruding into adjacent stroma/muscle tissue	Small	Electron-dense core with intact limiting membrane and electron-lucent halo	Sparse	Round nucleus with dispersed chromatin and prominent nucleolus, fine external basal lamina-like structure incorporating short runs of collagen fibrils, prominent SER, moderate amount of RER, lipid bodies, regions of cytoplasmic filaments, blunt-rounded protruding cell processes	0.6

within the cytoplasm of occasional cells.

Immunoelectron microscopy

Immunocytochemical staining with a primary

antibody to somatostatin revealed labelling within secretory granules of all tumour cell phenotypes. Antibody gold probe density overall was light but non-specific labelling was minimal allowing a high level of confidence in the specificity of positive labelling. Large

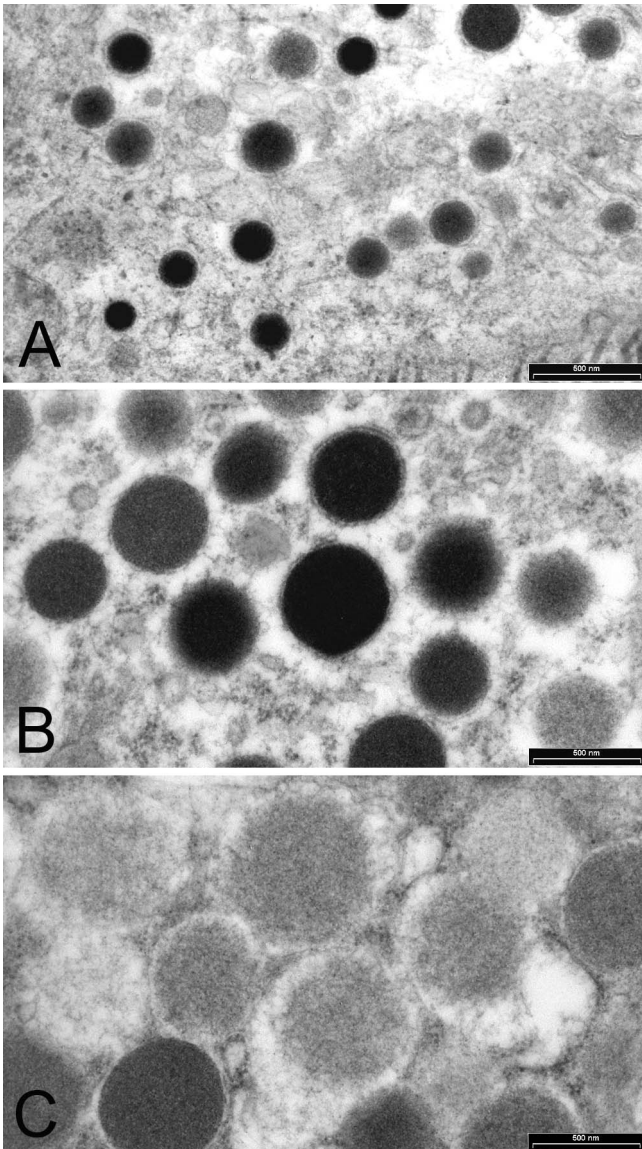


Fig. 8. Secretory granule development in somatostatinoma cells. **A.** Small 255-433 nm electron-dense granules of types 3 and 4 cells are thought to be early forms indicating an immature stage in the cell cycle. Note intact limiting membrane (Osmium, uranium and lead stain, x 28,000). **B.** Larger 625-815 nm electron-dense granules from a type 1 cell thought to represent the mature form of secretory granule. Limiting membrane still mostly intact (Osmium, uranium and lead stain, x 28,000). **C.** Larger 625-815 nm electron-pale granules typical of a type 2 cell. Limiting membrane is fragmented or missing and granule contents appear to be undergoing dispersal (Osmium, uranium and lead stain, x 28,000).

Table 2. Results of semi-quantitative morphometric analysis of somatostatinoma tumour cell secretory granule diameter.

Case	Large granule mean diameter (nm)	Std Dev	Small granule mean diameter (nm)	Std Dev
1	625	110	255	59
2	815	136	433	82

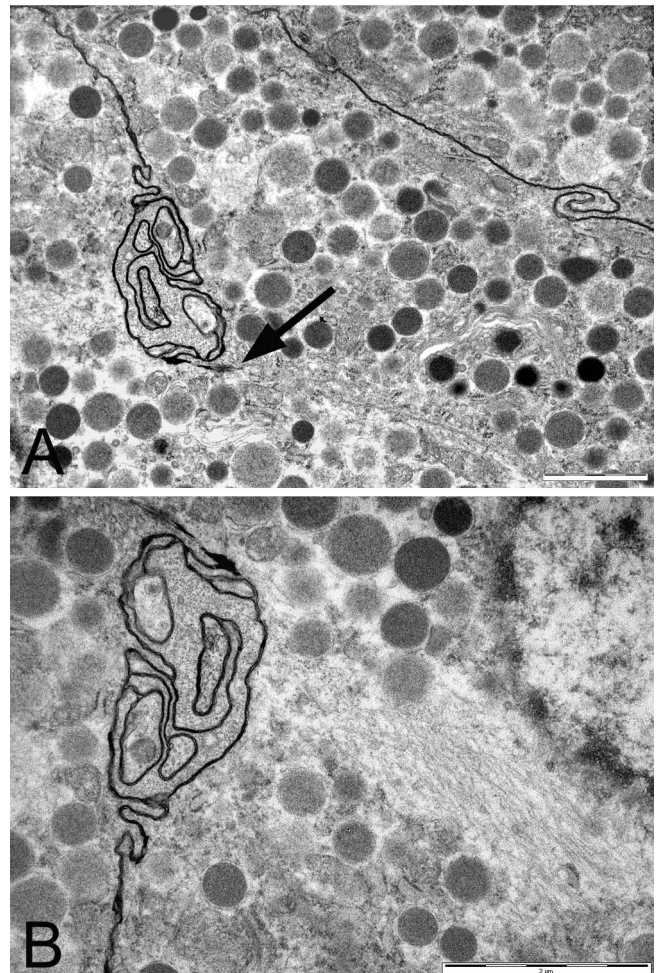


Fig. 9. Lateral intercellular space between type 1 tumour cells outlined by extracellular electron-dense material. **A.** Electron-dense material outlines interdigitating cell processes but terminates at a desmosome-like junction (arrow) (Osmium, uranium and lead stain, x 8,800). **B.** Higher power view of interdigitating cell processes (Osmium, uranium and lead stain, x 13,500).

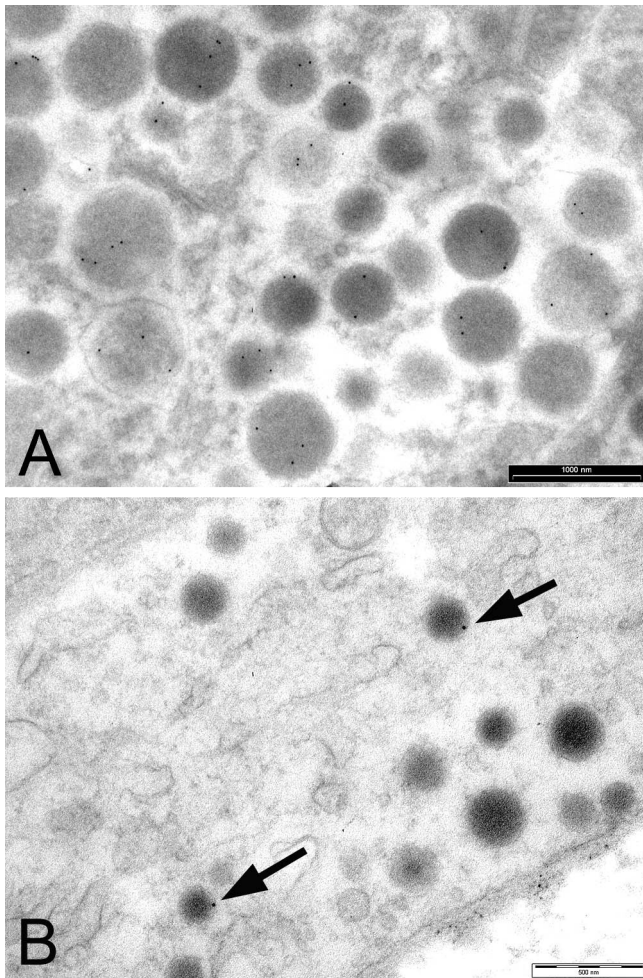


Fig. 10. Immunoelectron microscopy with *anti*-somatostatin immunogold labelling. **A.** 625-815 nm granules from a type 1 cell with positive labelling. Both electron-dense and less electron-dense forms of granules are labelled (Osmium and uranium counterstain, x 18,000). **B.** Smaller 255-433 nm granules from a type 3 cell with positive labelling (arrows) (Osmium and uranium counterstain, x 28,000).

granules of type 1 and 2 cells commonly contained 4 - 8 gold probes each (Fig. 10) whereas small granules of type 3 and 4 cells generally displayed 1 or 2 gold particles per granule (Fig. 10). Negative control sections incubated without primary antibody were clear of colloidal gold probes (not shown).

Discussion

Somatostatinomas are comparatively rare neuroendocrine neoplasms comprising less than 1% of gastropancreatic neuroendocrine neoplasms (Dayal and Ganda, 1991). The first case of duodenal somatostatinoma was reported by Kaneko et al. (1979) and since then more than a hundred cases have been described of which 46.8% were located in the pancreas,

about 15-20% of cases in the duodenum. Duodenal somatostatinomas have not been reported to be associated with the somatostatinoma syndrome of diabetes mellitus, steatorrhoea and cholelithiasis (Dayal and Ganda, 1991; Mao et al., 1995; House et al., 2002).

In the gastrointestinal tract somatostatinomas are thought to arise from pluripotent Delta-cells (D-cells). Somatostatin producing D-cells are present in the gastrointestinal tract, pancreas and central nervous system. In the gut they are most abundant in the more proximal parts in the epithelial lining of the crypts and dispersed in Brunner glands. The D-cells are argentaffin negative and not demonstrated by Grimelius or Sevier-Munger stains. They exhibit argyrophilia by the Hellerstorm-Hellman technique (Dayal and Ganda, 1991). Ultrastructurally, D-cells have been reported to contain predominantly 250-400nm diameter granules of varying electron density including dense core granules (Polak and Bloom, 1986; Kainuma et al., 1996) with characteristic electron-lucent or pale halo. Duodenal somatostatinomas are frequently but not invariably associated with Type I neurofibromatosis, whereas those pancreatic somatostatinomas may be associated with the somatostatinoma syndrome, either in full or partial manifestation depending on their secretory activity or their biological active by-products. Polypeptides produced by somatostatinomas are heterogenous; some of the peptides have less reactivity than other forms, which to some extent explains the differences in the clinical syndrome manifestations. It would seem that to get a better idea of the clinicopathological correlation an analysis of the isoforms of the secretions in the serum of patients should be carried out. It is of interest to mention that tumours other than somatostatinomas such as small cell carcinoma of the lung and medullary carcinoma of the thyroid may produce somatostatin although not in sufficiently large amounts or of significant biological activity to cause symptoms (Dayal and Ganda, 1991).

Histologically, somatostatinomas are usually made up of acinar or glandular structures with little sign of cellular pleomorphism, mitoses, necrosis or other features of malignancy. Psammoma bodies are a consistent but not specific feature of this neoplasm. The glandular structures are lined by positive PAS diastase resistant cells which are cuboidal, bland and uniform with granular eosinophilic cytoplasm. The nuclei are usually small and nucleoli are inconspicuous.

Somatostatinomas show positive immunohistochemical staining for epithelial markers, cytokeratin, neurone specific enolase, synaptophysin, chromogranin and somatostatin. Electron microscopic features include variable sized dense core membrane-bound granules with varying electron-density. These are not diagnostic and are a general feature of normal and neoplastic neurosecretory cells.

Our two patients aged 37 and 54 years are in the age group where somatostatinomas usually occur. The mean age of occurrence is 54 years with a slight predominance to females. The tumour in Case 1 occurred in the

duodenum, and is associated with Type I neurofibromatosis and cholecystitis but not the full somatostatinoma syndrome. Neurofibroma was first detected in the gall bladder following cholecystectomy for cholangitis and in the duodenum as a collision tumour with somatostatinoma.

Tanaka et al. studied 31 cases of duodenal somatostatinoma and reviewed the literature (Tanaka et al., 2000). It would appear that the size of the neoplasm is important in determining the biological behaviour and prognosis, whereas the patient's age, gender, whether it is associated with neurofibromatosis and the site of the tumour are not critical. Somatostatinomas of any size may metastasise. Most tumours are 3-6 μm in diameter but those over 20 mm have a higher risk of metastasis and those over 30 mm have a high chance of metastasis at the time of diagnosis. However, even small tumours of 8 mm have been known to metastasise, whereas tumours as large as 30 mm have not metastasised.

In the duodenum they are regarded as neoplasms of uncertain malignant potential. However, regardless of their biological malignant potential, their location in such a vital site means that they will invariably cause symptoms by compressing or infiltrating surrounding structures. It has been reported that about 20% are clearly malignant and over 60% have synchronous or metastatic disease at the time of diagnosis (House et al., 2002). Common sites of metastasis include regional lymph nodes, liver, bones, skin, ovaries and thyroid gland. The collision tumour in Case 1 of the present study is a chance occurrence. The two tumours collided, growing together as a single mass contributing to the overall size of 35 mm and the obstructive symptoms. The somatostatinoma was the larger component comprising two thirds of the collision tumour and was therefore estimated to be 20 mm in diameter, still having a significant risk of metastasis but not as high as if the tumour were to be 35 mm in diameter. The histological features of components of the two tumours were readily distinguished with routine and immunoperoxidase stains. In our patient, the previously established diagnosis of neurofibromatosis and the well-known association of this neoplasm with Type I neurofibromatosis was helpful. However, it was important to remember that a gastrointestinal tumour may occur at this site and should not be mistaken for a neurofibroma.

A gastrointestinal tumour (GIST) at this site can be distinguished from a neurofibroma by demonstrating negative staining for S-100 and positive staining for CD117 and CD34. The somatostatinoma component of the tumour can be distinguished from ampullary carcinoid or adenocarcinoma by the appropriate immunohistochemical stains. Another significant point to make about this collision tumour is that if the biopsy tissue only contained the spindle cell component the diagnosis of somatostatinoma may not have been established.

There are only a few reports detailing the ultrastructural pathology of somatostatinoma (Ranaldi et

al., 1988). We therefore set out to conduct a more detailed study of the ultrastructural features to find specific or unusual features, and especially to find out if somatostatinoma possess ultrastructural characteristics that are different from other neuroendocrine neoplasms. We were also interested to find out if granules and other cellular substructures show qualitative or quantitative changes that help in their diagnosis and improve our understanding of their secretory activity and how this would relate to the associated clinical syndrome. We applied immunoelectron microscopy to try to localise somatostatin sites at the subcellular level, to find out if granule appearance correlates with secretory storage, or secretion.

We found that somatostatinoma cells contain cytoplasmic granules of variable size and electron-density resembling secretory granules of the islet D-cell. We were able to identify four different types of tumour cells based on their general ultrastructure and the density, distribution and size of their secretory granules. The majority of tumour cells which we called type 1 contained generally electron-dense granules with a mean diameter of 625-815 nm. These were significantly larger than the 300-350 nm size usually reported for normal D-cells (Varndell et al., 1986; Ranaldi et al., 1988; Ghadially, 1997). However, alteration in granule size and morphology is regarded as a common occurrence in neoplastic transformation (Ghadially, 1997).

The minor subpopulation of neoplastic cells with smaller secretory granules we identified as types 3 and 4 were located mainly in the periphery of tumour acini. Similar cells have been described in somatostatinoma by others (Varndell et al., 1986; Ranaldi et al., 1988) and were thought by one group (Varndell et al., 1986) to correspond to the neoplastic equivalent of the extra-islet D1-cell. They displayed typical dense core granules commonly seen in many types of neuroendocrine neoplasms, with an electron-lucent halo and intact limiting membrane. Taccagni et al. reported the presence of small 150-370 nm granules admixed with typical large, electron-pale secretory granules in single somatostatinoma cells (Taccagni et al., 1986). We also noted cells containing predominantly large granules that also contained some small granules suggesting that the small granules may be precursors of the large granules and in turn that, cells which contain predominantly small granules may represent cells at a more immature stage. We postulate that Type 1 and 2 cells with large granules represent the mature phenotype of somatostatinoma cells. The variation in secretory granule size may simply be a reflection of changes in the packaging or concentration of peptide hormone (Ghadially, 1997). The breakdown of the limiting membranes of the larger somatostatin granules appears to be a feature of full maturation and impending release of the granule contents. Immunoelectron microscopy employing polyclonal antibody to somatostatin showed positive labelling in secretory granules of all sizes and electron-density further supporting the above interpretation.

There was no detectable difference in labelling intensity between the various types of granules encountered supporting the view that classifying D-cell secretory granules into subgroups based on their electron-density is not warranted (Varndell et al., 1986). However, as we have observed significant variation in tumour cell morphology particularly with regard to granule types, we have persisted in dividing the cells into different subtypes and quantifying their relative numbers in the tumour. This approach may be helpful with diagnosis when limited tissue is available for examination by providing a description of the spectrum of somatostatinoma cell appearances possible. Analysis of phenotypic variation may also shed some light on tumour behaviour. Features of type 2 cells such as nuclear shape and density of nucleoplasm suggested that these were older cells possibly destined for necrosis that may be "leaky" to somatostatin. The predominantly peripheral location of type 3 cells suggested that cell division occurs mainly at the margins of tumour acini. It is also interesting to note that type 4 cells that contained few neurosecretory granules appeared to be the most capable of penetrating the surrounding stroma and therefore may represent the invasive stage of the tumour cell growth cycle.

We found psammoma bodies to be common within the lumen of neoplastic glands in both tumours. These bodies exhibited a concentric crystalline structure similar to that described by other authors (Taccagni et al., 1986; Ranaldi et al., 1988). One of these authors demonstrated that the crystalline material contained calcium and phosphorous (Ranaldi et al., 1988). They also described similar crystalline material in the cytoplasm of neighbouring cells and the presence of lipofuscin-like material forming a psammoma body core raising the possibility that some psammoma body material may be formed within somatostatinoma cells before being expelled into the luminal space. We noted the presence of some electron-dense core material in psammoma bodies but did not make any specific attempt to confirm this to be lipofuscin. We also observed some similar intracytoplasmic crystalline deposits in neighbouring cells. However, there was no evidence to suggest externalisation of this material from these cells played a role in psammoma body formation in the luminal space.

The concentric layering of crystalline material in psammoma bodies suggested sequential deposition of material occurs within the luminal space. The electron-dense staining of the lateral intercellular space also supports the hypothesis that aberrant secretion of calcium rich material into the luminal space may be occurring. We therefore support the concept of luminal formation of psammoma bodies by a process of dystrophic calcification, a view that has been proposed by others (Ranaldi et al., 1988).

Our experience with these two cases of somatostatinoma is that the diagnosis is relatively straightforward when they exhibit the classical histological and immunohistochemical features. In

frozen section diagnosis and in instances where the tissue is very small the diagnosis may be problematic. Where there is a history of neurofibromatosis or somatostatinoma syndrome, somatostatinoma must always be considered as a probable diagnosis. The collision of somatostatinoma and neurofibroma was only recognised after the surgical removal of the tumour. It did not pose any diagnostic difficulties and its only significance is in that the benign neurofibroma component should not be included in the assessment of the overall size of the tumour to determine malignant potential. If the neoplasm does not have classical features of somatostatinoma, adenoma, carcinoma, metastatic carcinoma, other neoplasms aforementioned in the text, depending what features are present, will have to be considered in the differential diagnosis. Immunohistochemistry is helpful in deriving the most likely diagnosis. Electron microscopic studies reveal that there may be four somatostatinoma cell phenotypes based on location within the tumour and the size, number and electron-density of their secretory granules. If we are correct in predicting that types 1 and 2 cells are functionally mature cells whereas types 3 and 4 cells are functionally immature cells, it may be possible to predict that those tumours with a predominant content of types 1 and 2 cells are more likely to be associated with the somatostatinoma syndrome and those tumours with more than expected type 3 and 4 cells are likely to behave in a more aggressive manner.

References

- Dayal Y. and Ganda O.P. (1991). Somatostatin producing tumours. In: Endocrine pathology of the gut and pancreas. 1st ed. Dayal Y. (ed). CRC Press. Boca Raton, FL. pp 241-277.
- Ghadially F.N. (1997). Golgi complex and secretory granules. In: Ultrastructural pathology of the cell and matrix. 4th ed. Chapter 4. Butterworth-Heinemann. Boston. pp 343-432.
- House M.G., Yeo C. and Schulick R.D. (2002). Peri-ampullary pancreatic somatostatinoma. *Ann. Surg. Oncol.* 9, 869-874.
- Johannessen J.V. (1973). Rapid processing of kidney biopsies for electron microscopy. *Kidney Int.* 3, 46-52.
- Kainuma O., Ito Y., Taniguchi T., Shimizu T., Nakada H., Date Y. and Hara T. (1996). Ampullary somatostatinoma in a patient with Von Recklinghausen's disease. *J. Gastroenterol.* 31, 460-464.
- Kaneko H., Yanaiharu N., Ito S., Kusumoto Y., Fujita T., Ishikawa S., Sumida T. and Sekiya M. (1979). Somatostatinoma of the duodenum. *Cancer* 44, 2273-2279.
- Mao C., Shah A., Hanson D.J. and Howard J.M. (1995). Von Recklinghausen's disease associated with duodenal somatostatinoma: contrast of duodenal versus pancreatic somatostatinoma. *J. Surg. Oncol.* 59, 67-73.
- Polak J.M. and Bloom S.R. (1986). Somatostatin localization in tissues. *Scan. J. Gastroenterol. Suppl.* 119, 11-21.
- Ranaldi R., Bearzi I., Cinti S. and Suraci V. (1988). Ampullary somatostatinoma; an immunohistochemical and ultrastructural study. *Pathol. Res. Pract.* 183, 8-16.
- Stirling J.W. and Graff P.S. (1995). Antigen unmasking for immunoelectron microscopy: labelling is improved by treating with

Somatostatinoma collision tumour

- sodium ethoxide or sodium metaperiodate, then heating on retrieval medium. *J. Histochem. Cytochem.* 43, 115-123.
- Taccagni G.L., Carlucci M., Sironi M., Cantaboni A. and Di Carlo V. (1986). Duodenal somatostatinoma with psammoma bodies: an immunohistochemical and ultrastructural study. *Am. J. Gastroenterol.* 81, 33-37.
- Tanaka S., Yamasaki S., Matsushita H., Ozawa Y., Kurosaki A., Takeuchi K., Hosihara Y., Doi T., Watanabe G. and Kawaminami K. (2000). Duodenal somatostatinoma; a case report and review of 31 cases with special reference to the relationship between tumour size and metastasis. *Pathol. Int.* 50, 1048-1053.
- Varndell I.M., Sikri K.L., Hennessey R.J., Kalina M., Goodman R.H., Benoit R., Diani A.R. and J.M. (1986). Somatostatin-containing D cells exhibit immunoreactivity for rat somatostatin cryptic peptide in six mammalian species; an electron-microscopical study. *Cell Tissue Res.* 246, 197-204.

Accepted May 17, 2006